

Effect of nonrelativistic interface Hamiltonian on optical transitions in broken-gap heterostructures

I. Semenikhin and A. Zakharova

Institute of Physics and Technology of the Russian Academy of Sciences, Nakhimovskii Avenue 34, Moscow 117218, Russia

K. A. Chao

Department of Physics, Lund University, Sölvegatan 14A S-22362 Lund, Sweden

and Department of Physics, Chemistry and Biology, Linköping University, S-58283 Linköping, Sweden

(Received 12 November 2007; revised manuscript received 31 January 2008; published 13 March 2008)

Using the Burt-Foreman envelope function theory and an eight-band $\mathbf{k}\cdot\mathbf{p}$ model, we have extended our previous work [Semenikhin *et al.* Phys. Rev. B **76**, 035335 (2007)] on optical transitions in InAs/GaSb quantum wells grown along the [001] direction by completing the interface Hamiltonian with the inclusion of its nonrelativistic part. We found a substantial contribution of the nonrelativistic term to the originally forbidden spin-flip optical transitions. However, this nonrelativistic term produces only a minor modification of the lateral optical anisotropy.

DOI: [10.1103/PhysRevB.77.113307](https://doi.org/10.1103/PhysRevB.77.113307)

PACS number(s): 73.21.Ac, 73.21.Fg, 73.40.Kp

Spin split of energy levels and spin dependent intersubband optical transitions caused by linearly polarized light in semiconductor quantum wells and superlattices¹⁻⁷ exhibit specific effects if the systems are of InAs/GaSb broken-gap type where the InAs conduction band overlaps with the GaSb valence band. When the lowest electron level in the InAs layer lies below the highest hole level in the GaSb layer, existing hybridization gap in in-plane dispersion was observed⁸⁻¹¹ and analyzed theoretically.¹²⁻¹⁸ The lateral anisotropy of spin-dependent intersubband optical absorption of light linearly polarized along the [11] and the $[1\bar{1}]$ directions was also investigated both theoretically and experimentally.¹⁹⁻²² The relevant mechanisms are spin-orbit interaction, structural inversion asymmetry (SIA), bulk inversion asymmetry (BIA), and low symmetry of interfaces which can be described by a specific interface Hamiltonian (IH).

The IH contains a relativistic part²³ and a nonrelativistic part.^{24,25} In our earlier paper²⁶ it was shown that the BIA and the relativistic IH term can activate the initially forbidden intersubband optical transitions in an AlSb/InAs/GaSb/AlSb broken-gap quantum well caused by linearly polarized light. Also the effects of the BIA and the relativistic IH term on lateral optical anisotropy for the transitions caused by the light linearly polarized along the [11] and $[1\bar{1}]$ directions were studied in the same paper. The nonrelativistic IH term was not included in Ref. 26 because the strength of this term was not known quantitatively. In the present work we will first calculate the nonrelativistic IH term and then study its additional effect on spin-dependent optical matrix elements and lateral optical anisotropy. To be consistent, we will use the same notations as those in Ref. 26, and the reader can refer to it for details.

We will consider the AlSb/InAs/GaSb/AlSb quantum well grown on GaSb along the [001] direction which we take as the z axis. In the plane perpendicular to [001], the [10] direction is the x axis, and the [01] direction is the y axis. The eight-band Hamiltonian around Γ point

$$\hat{H} = \begin{pmatrix} \hat{H}_4 & 0 \\ 0 & \hat{H}_4 \end{pmatrix} + \hat{H}_{so} + \hat{H}_\epsilon + \hat{H}_{ek} + \hat{H}_B + \hat{H}_k \quad (1)$$

is constructed with respect to the set of basis functions

$$S\uparrow, X\uparrow, Y\uparrow, Z\uparrow, S\downarrow, X\downarrow, Y\downarrow, Z\downarrow \quad (2)$$

as in Ref. 26. In Eq. (1), \hat{H}_4 is a 4×4 matrix, which depends on the conduction and valence band edges, the momentum operators, the interband momentum matrix elements, and the modified Luttinger parameters. \hat{H}_{so} is the spin-orbit interaction and \hat{H}_ϵ the strain Hamiltonian, both of which are independent of the momentum operators. The explicit forms of \hat{H}_4 , \hat{H}_{so} , and \hat{H}_ϵ are given in Ref. 17. The next two terms \hat{H}_{ek} and \hat{H}_B are due to BIA, and the last matrix \hat{H}_k is the interface Hamiltonian. Although these last three terms \hat{H}_{ek} , \hat{H}_B , and \hat{H}_k are given in Ref. 26, here we will present the exact form of the nonrelativistic part of \hat{H}_k since its effect on optical properties is the central theme of this paper.

The complete IH matrix \hat{H}_k contains a relativistic part \hat{H}_k^R and a nonrelativistic part \hat{H}_k^{NR} . The expression of \hat{H}_k^{NR} with respect to the basis set given by Eq. (2) can be found in Ref. 25 and has the form

$$\hat{H}_k^{NR} = \begin{pmatrix} \hat{H}_{k0}^{NR} & 0 \\ 0 & \hat{H}_{k0}^{NR} \end{pmatrix}, \quad (3)$$

where

$$\hat{H}_{k0}^{NR} = \left\{ \sum_j \Omega_j \delta(z - z_j) \right\} \begin{pmatrix} 0 & 0 & 0 & 0 \\ 0 & 0 & 1 & 0 \\ 0 & 1 & 0 & 0 \\ 0 & 0 & 0 & 0 \end{pmatrix}. \quad (4)$$

Ω_j is the coupling constant for the light-heavy-hole mixing at the j th interface located at $z = z_j$, and its value depends on materials. In this paper we use the pseudopotential

approach²⁵ to calculate Ω_j for the planar abrupt interfaces AlSb/InAs, InAs/GaSb, and GaSb/AlSb.

The Schrödinger equation $\hat{H}\Psi_i = E_i\Psi_i$, where Ψ_i is the multicomponent envelope function and E_i the corresponding energy, is solved self-consistently together with the Poisson equation, also taking into account the lattice-mismatched strain. Knowing the envelope functions, the optical matrix elements are obtained as^{27,28}

$$M = (2m)^{1/2} \langle \Psi_{\mathbf{k}} | \mathbf{e} \cdot \hat{\mathbf{v}} | \Psi_{\mathbf{l}} \rangle, \quad (5)$$

where m is the free electron mass, $\hat{\mathbf{v}}$ the velocity operator, and \mathbf{e} the unit vector of light polarization. For optical transitions between the α subband and the β subband, let us introduce a quantity

$$I_{\alpha\beta}(\mathbf{e}, \mathbf{k}_{\parallel}) = \sum_{i,j} |M_{ij}(\mathbf{e}, \mathbf{k}_{\parallel})|^2, \quad (6)$$

where i runs over the states in the α subband and j runs over the states in the β subband. In terms of this quantity, the polarization, which characterizes the lateral optical anisotropy, can be defined as

$$\lambda_{\alpha\beta} = \frac{I_{\alpha\beta}(\mathbf{e}_2, \mathbf{k}_{\parallel}) - I_{\alpha\beta}(\mathbf{e}_1, \mathbf{k}_{\parallel})}{I_{\alpha\beta}(\mathbf{e}_2, \mathbf{k}_{\parallel}) + I_{\alpha\beta}(\mathbf{e}_1, \mathbf{k}_{\parallel})}, \quad (7)$$

where the vector \mathbf{e}_1 is along the $[11]$ direction, and the vector \mathbf{e}_2 along the $[1\bar{1}]$ direction. For numerical calculations, the thickness of each of the four layers in the AlSb/InAs/GaSb/AlSb quantum well is set as 10 nm. Furthermore, the quantum well itself is sandwiched between two p -doped GaSb contact layers with acceptor concentration $2 \times 10^{18} \text{ cm}^{-3}$. All parameter values needed for the calculation, as well as the detailed numerical procedure, can be found in Ref. 26.

We derive the values of the parameters Ω_j with a pseudopotential approach, using all pseudopotential form factors given in Ref. 29, except for the form factor V_0^S which we adopt $V_0^S = 0 \text{ Ry}$ for InAs and AlSb, and $V_0^S = 0.02 \text{ Ry}$ for GaSb.³⁰ Our so-obtained values are $\Omega = 0.034 \text{ eV \AA}$ for the AlSb/InAs heterojunction, $\Omega = 0.23 \text{ eV \AA}$ for the InAs/GaSb heterojunction, and $\Omega = -0.26 \text{ eV \AA}$ for the GaSb/AlSb heterojunction.

For the convenience of presenting and discussing our numerical results, we will define a partial Hamiltonian

$$\hat{H}_P = \begin{pmatrix} \hat{H}_A & 0 \\ 0 & \hat{H}_4 \end{pmatrix} + \hat{H}_{so} + \hat{H}_{\epsilon} + \hat{H}_{\epsilon k} + \hat{H}_B + \hat{H}_k^R, \quad (8)$$

which does not include the nonrelativistic interface Hamiltonian, and was studied in detail in Ref. 26. In the following discussion we will focus on the difference between the results obtained with the full Hamiltonian \hat{H} and the partial Hamiltonian \hat{H}_P .

For the above specified InAs/GaSb quantum well, the subband dispersions derived with \hat{H} differ from those derived with \hat{H}_P only quantitatively with a slightly larger spin split of levels. According to their wave function properties at the zone center ($\mathbf{k}_{\parallel} = 0$), the levels which are relevant to the

present work are labeled as $1e$ and $2e$ for the electronlike states, $1hh$, $2hh$, and $3hh$ for the heavy-holelike states, and $1lh$ for the light-holelike state. From the bottom of the quantum, their order at $\mathbf{k}_{\parallel} = 0$ is $3hh$, $1lh$, $2hh$, $1e$, $1hh$, and $2e$. Since the $1e$ level lies below the $1hh$ level at the zone center, a hybridization gap is created between them at $k_{\parallel} \approx 0.1 \text{ nm}^{-1}$. This hybridization leads to unusual behavior of optical transitions between not only the states of $1e$ and $2e$ subbands but also the states of $1hh$ and $2e$ subbands, the study of which was initiated in Ref. 26 and will be completed in the present work. Consequently, we will use the same notations as in Ref. 26 to label the two spin-split dispersion branches of each subband: in the region of small k_{\parallel} , the lower branch is assigned with a subscript a and the upper branch with a subscript b .

The numerical calculations were performed with light polarized along the growth direction $[001]$ or in the plane of the structure. It was shown earlier²⁶ that the interesting phenomena in spin-flip transition occur if the in-plane wave vector \mathbf{k}_{\parallel} of the initial state is along a high symmetry direction. Therefore, for all our calculated optical matrix elements presented in the form $|M_0|^2 \equiv |\hbar M / \sqrt{2m}|^2$ in Figs. 1 and 2, the \mathbf{k}_{\parallel} of the initial state is along the $[10]$ direction.

The numerical results of $|M_0|^2$ are given in Fig. 1 for $1e$ - $2e$ transitions [Figs. 1(a) and 1(b)] and $1hh$ - $2e$ transitions [Figs. 1(c) and 1(d)]. Figures 1(a) and 1(c) are derived from \hat{H}_P and Figs. 1(b) and 1(d) from \hat{H} . In Figs. 1(a) and 1(b), the solid (or dashed) curve is for the $1e_b$ - $2e_a$ (or $1e_a$ - $2e_b$) transition which is a spin-flip process near the zone center, while the dotted (or dash-dotted) curve is for the $1e_a$ - $2e_a$ (or $1e_b$ - $2e_b$) transition for which the spin orientation is conserved around $k_{\parallel} = 0$. By comparing the corresponding curves in Figs. 1(a) and 1(b), we see that the nonrelativistic part \hat{H}_k^{NR} of the IH \hat{H}_k increases further the intensity of the spin-flip $1e$ - $2e$ optical transition, which is already enhanced by the BIA term and the \hat{H}_k^{NR} term in \hat{H}_P as proved in Ref. 26. Consequently, in this case the contributions of BIA, relativistic IH, and nonrelativistic IH to the optical matrix element M are additive.

However, the situation is quite different for the $1hh$ - $2e$ optical transitions, as shown in Figs. 1(c) and 1(d), where the solid (or dashed) curve is for the spin-flip $1hh_b$ - $2e_a$ (or $1hh_a$ - $2e_b$) transition and the dotted (or dash-dotted) curve is for the spin conserved $1hh_a$ - $2e_a$ (or $1hh_b$ - $2e_b$) transition. The value of $|M_0|^2$ for each spin-flip transition in Fig. 1(d) derived with \hat{H} is smaller than the corresponding value in Fig. 1(c) derived with \hat{H}_P . This result strongly suggests that the contribution of \hat{H}_k^{NR} to M is substantial, and is not additive to the combined contribution of BIA and \hat{H}_k^R . To confirm this conjecture, we removed the BIA term and \hat{H}_k^R from \hat{H} , and then calculated $|M_0|^2$ once again to check how Fig. 1(d) changes. The result is shown in Fig. 2 with the same notation for the four curves as that in Fig. 1(d). The substantial contribution of \hat{H}_k^{NR} to M is clearly seen.

Finally we investigate the effect of \hat{H}_k^{NR} on lateral optical anisotropy. For the in-plane wave vector \mathbf{k}_{\parallel} of the initial state along the $[10]$ direction, the polarization calculated with Eq.

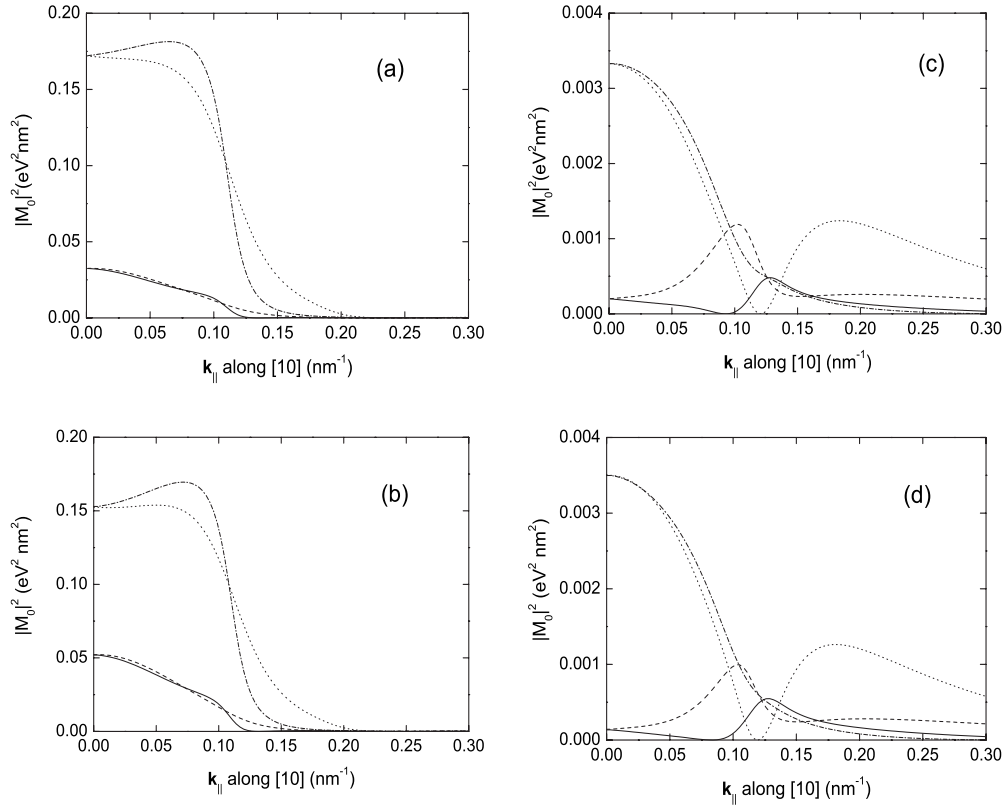


FIG. 1. Square of the absolute value of the optical matrix element. (a) and (b) Transition from a state in the $1e$ subband to a state in the $2e$ subband, with light polarized along the $[001]$ direction. Solid, dashed, dotted, and dash-dotted curves in each panel correspond to the $1e_b-2e_a$, $1e_a-2e_b$, $1e_a-2e_a$, and $1e_b-2e_b$ transitions, respectively. (c) and (d) Transition from a state in the $1hh$ subband to a state in the $2e$ subband, with light polarized along the $[10]$ direction. Solid, dashed, dotted, and dash-dotted curves in each panel correspond to the $1hh_b-2e_a$, $1hh_a-2e_b$, $1hh_a-2e_a$, and $1hh_b-2e_b$ transitions, respectively. (a) and (c) are obtained with the partial Hamiltonian \hat{H}_p , and (b) and (d) are obtained with the full Hamiltonian \hat{H} .

(7) is shown in Fig. 3. The total polarization derived with \hat{H} is plotted as a solid curve for the $1hh-2e$ transitions, and as a dotted curve for the $1e-2e$ transitions. While using \hat{H}_p to perform a similar calculation, with the effect of \hat{H}_k^{NR} neglected, the solid curve becomes the dashed curve, and the dotted curve turns into the dash-dotted curve. Our numerical

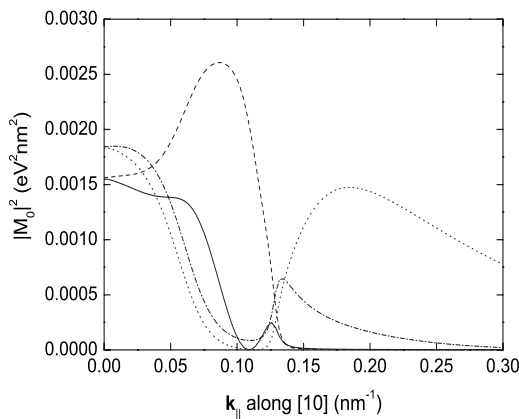


FIG. 2. The same as Fig. 1(d), but obtained with the neglect of the BIA term and the \hat{H}_k^{NR} in the full Hamiltonian \hat{H} .

results indicate that the effect of \hat{H}_k^{NR} on lateral optical anisotropy is weak, but nevertheless not negligible.

In summary, we have added the \hat{H}_k^{NR} term to the previously studied Hamiltonian²⁶ and have performed a self-

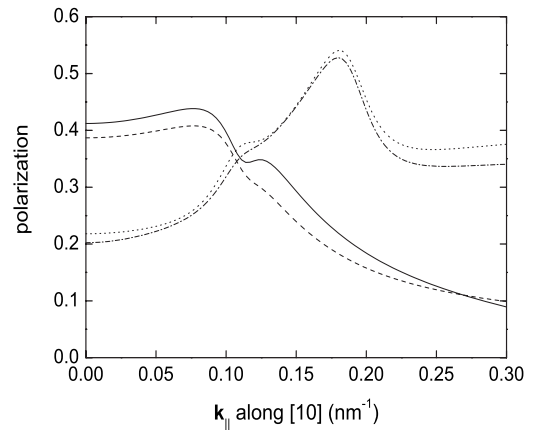


FIG. 3. Polarization for k_{\parallel} along the $[10]$ direction. Solid and dotted curves, which are calculated with \hat{H} , are for the $1hh-2e$ and the $1e-2e$ transitions, respectively. The corresponding transitions calculated with \hat{H}_p are plotted in dashed and dash-dotted curves.

consistent calculation to demonstrate the effect of \hat{H}_k^{NR} on optical matrix elements and lateral optical anisotropy in InAs/GaSb quantum wells. We found a substantial contribution of \hat{H}_k^{NR} to the originally forbidden spin-flip optical transitions. On the other hand, there is only a minor modification of the lateral optical anisotropy. Hence the main contribution to the latter effect results from the BIA, which induces the localized interface contribution to the optical matrix elements due to the material dependent Kane's B -parameter.²⁶ We believe that the originally forbidden spin-flip optical

transitions, which are substantial when the electron and hole states are strongly hybridized, may cause the additional peaks of absorption of linearly polarized light in broken-gap heterostructures. The experimental observation of our theoretical findings is possible by performing proper measurements of the optical transitions between the states of the $1hh$ and $2e$ subbands, as well as between the states of the $1e$ and $2e$ subbands.

This work was financially supported by the Russian Foundation for Basic Research under Grant No. 07-02-00680-a.

-
- ¹E. I. Rashba, Sov. Phys. Solid State **2**, 1109 (1960); Yu. A. Bychkov and E. I. Rashba, JETP Lett. **39**, 78 (1984).
²J. Luo, H. Muneke, F. F. Fang, and P. J. Stiles, Phys. Rev. B **38**, 10142 (1988); Phys. Rev. B **41**, 7685 (1990).
³M. Silver, W. Batty, A. Ghiti, and E. P. O'Reilly, Phys. Rev. B **46**, 6781 (1992).
⁴O. Mauritz and U. Ekenberg, Phys. Rev. B **55**, 10729 (1997).
⁵Yia-Chung Chang and J. N. Schulman, Phys. Rev. B **31**, 2069 (1985).
⁶Bang-fan Zhu and Yia-Chung Chang, Phys. Rev. B **50**, 11932 (1994).
⁷R. J. Warburton, C. Gauer, A. Wixforth, J. P. Kotthaus, B. Brar, and H. Kroemer, Phys. Rev. B **53**, 7903 (1996).
⁸M. J. Yang, C. H. Yang, B. R. Bennett, and B. V. Shanabrook, Phys. Rev. Lett. **78**, 4613 (1997).
⁹M. Lakrimi, S. Khym, R. J. Nicholas, D. M. Symons, F. M. Peeters, N. J. Mason, and P. J. Walker, Phys. Rev. Lett. **79**, 3034 (1997).
¹⁰L. J. Cooper, N. K. Patel, V. Drouot, E. H. Linfield, D. A. Ritchie, and M. Pepper, Phys. Rev. B **57**, 11915 (1998).
¹¹A. J. L. Poulter, M. Lakrimi, R. J. Nicholas, N. J. Mason, and P. J. Walker, Phys. Rev. B **60**, 1884 (1999).
¹²M. Altarelli, Phys. Rev. B **28**, 842 (1983).
¹³Y. Naveh and B. Laikhtman, Appl. Phys. Lett. **66**, 1980 (1995).
¹⁴R. Magri, L. W. Wang, A. Zunger, I. Vurgaftman, and J. R. Meyer, Phys. Rev. B **61**, 10235 (2000).
¹⁵E. Halvorsen, Y. Galperin, and K. A. Chao, Phys. Rev. B **61**, 16743 (2000).
¹⁶A. Zakharova, S. T. Yen, and K. A. Chao, Phys. Rev. B **64**, 235332 (2001).
¹⁷A. Zakharova, S. T. Yen, and K. A. Chao, Phys. Rev. B **66**, 085312 (2002).
¹⁸I. Vurgaftman and J. R. Meyer, Phys. Rev. B **70**, 115320 (2004).
¹⁹F. Fuchs, J. Schmitz, J. D. Rultson, P. Koidl, R. Heintz, and A. Hoffmann, Superlattices Microstruct. **16**, 35 (1994).
²⁰O. Krebs and P. Voisin, Phys. Rev. B **61**, 7265 (2000).
²¹L. W. Wang, S. H. Wei, T. Mattila, A. Zunger, I. Vurgaftman, and J. R. Meyer, Phys. Rev. B **60**, 5590 (1999).
²²E. L. Ivchenko and M. O. Nestoklon, Phys. Rev. B **70**, 235332 (2004).
²³Bradley A. Foreman, Phys. Rev. Lett. **86**, 2641 (2001).
²⁴E. L. Ivchenko, A. Yu. Kaminski, and U. Rössler, Phys. Rev. B **54**, 5852 (1996).
²⁵Bradley A. Foreman, Phys. Rev. Lett. **81**, 425 (1998).
²⁶I. Semenikhin, A. Zakharova, K. Nilsson, and K. A. Chao, Phys. Rev. B **76**, 035335 (2007).
²⁷J. N. Schulman and Yia-Chung Chang, Phys. Rev. B **31**, 2056 (1985).
²⁸R. Winkler, M. Merkler, T. Darnhofer, and U. Rössler, Phys. Rev. B **53**, 10858 (1996).
²⁹Marvin L. Cohen and T. K. Bergstresser, Phys. Rev. **141**, 789 (1966).
³⁰Jian-Bai Xia, Phys. Rev. B **39**, 3310 (1989).